Impacts of the aneurysm deformation induced by stent on hemodynamic of blood flow in saccular internal carotid artery aneurysms

RESEARCH ARTICLE | SEPTEMBER 26 2024

Impacts of the aneurysm deformation induced by stent on hemodynamic of blood flow in saccular internal carotid artery aneurysms

S. Valiallah Mousavi ; Mostafa Barzegar Gerdroodbary ; Amir Sabernaeemi ; Sajad Salavatidezfouli ; Peiman Valipour

AIP Advances 14, 095035 (2024)
https://doi.org/10.1063/5.0224235

Impacts of the aneurysm deformation induced by stent on hemodynamic of blood flow in saccular internal carotid artery aneurysms

Cite as: AIP Advances 14, 095035 (2024); doi: 10.1063/5.0224235
Submitted: 20 June 2024 • Accepted: 6 September 2024 •
Published Online: 26 September 2024

S. Valiallah Mousavi,[1,a] Mostafa Barzegar Gerdroodbary,[2] Amir Sabernaeemi,[3] Sajad Salavatidezfouli,[4] and Peiman Valipour[5]

AFFILIATIONS

[1] Department of Mechanical Engineering, Technical and Vocational University (TVU), Tehran, Iran
[2] Department of Electromechanical Engineering, C-MAST-Center for Mechanical and Aerospace Science and Technology, Universidade da Beira Interior, Covilha, Portugal
[3] Department of Space, Earth and Environment, Chalmers University of Technology, Gothenburg, Sweden
[4] Mathematics Area, MathLab, International School for Advanced Studies (SISSA), Trieste, Italy
[5] Department of Textile Engineering, Clothing and Fashion, Qaemshahr Branch, Islamic Azad University, Qaemshahr, Iran

[a] **Author to whom correspondence should be addressed:** vmousavi@tvu.ac.ir

ABSTRACT

Recognition of the aneurysm rupture risk after endovascular treatments is important for the evaluation of the applied treatment technique. In this paper, the role of the stent in the treatment of saccular internal carotid artery (ICA) aneurysm patients has been investigated to assess the performance of this endovascular technique in the reduction of bleeding possibility and hemorrhage. Hemodynamic studies have been performed to compare the main effective factors of wall shear stress, oscillatory index, and pressure on the aneurysm wall in different stages of the cardiac cycle. The computational technique of finite volume is used to model the pulsatile blood flow inside three different ICA patients. To simulate blood flow, the one-way fluid–solid interaction technique is considered for the interaction of the blood and vessel, and the Casson non-Newtonian model is applied for the modeling of the blood viscosity. The comparison of the velocity magnitude of deformed cases with the original also shows how the blood flow is limited by the deformation of the aneurysms. Aneurysm deformation induced by the stent reduces the blood flow rate into the sac section, and consequently, wall shear stress is decreased on the surface of aneurysms. Stent-induced straightening of the vessel shows superior performance in hemodynamic changes and could lower recurrence rates, while stenting may have negative impacts on hemodynamic alterations.

I. INTRODUCTION

Cerebral aneurysms are abnormal bulges or weak spots that develop in the walls of blood vessels within the brain, potentially posing a serious health risk due to the potential for rupture. Among the various treatment options available for patients with intracranial aneurysms, the use of stents to induce aneurysm deformation has emerged as a promising approach. This introduction aims to explore the concept of stent-induced aneurysm deformation and its potential efficacy in treating patients specifically with saccular cerebral aneurysms located in the internal carotid artery (ICA).[1–3]

Saccular cerebral aneurysms, also known as berry aneurysms, are the most common form of intracranial aneurysms, accounting for ~90% of cases. These aneurysms typically arise at the branching points of major cerebral arteries, with the ICA being a commonly affected vessel. Historically, treatment options for saccular ICA aneurysms have included surgical clipping and endovascular coiling. However, these methods have their limitations and may not always be suitable for all patients or anatomical configurations.[4,5]

The introduction of stent-assisted techniques in the management of cerebral aneurysms has provided an alternative approach that offers potential benefits. Stents, originally developed as flow

diverters, are now being utilized in a manner that induces aneurysm deformation, with the aim of reducing the risk of rupture and promoting long-term stability.[6–8]

The concept behind stent-induced aneurysm deformation lies in the physical interaction between the stent and the aneurysm itself. By deploying a stent across the neck or ostium of the aneurysm, blood flow within the aneurysm is altered, leading to changes in hemodynamics and subsequent aneurysm remodeling. The stent acts as a scaffold, promoting thrombus formation within the aneurysm sac, effectively sealing it off from circulating blood and reducing the risk of rupture.[9,10]

Several studies have shown promising results regarding the efficacy of stent-induced aneurysm deformation in the treatment of saccular ICA aneurysms. These studies have demonstrated a significant reduction in aneurysm size, increased rates of occlusion, and decreased rates of aneurysm rupture in patients treated with this technique. Furthermore, stent-assisted coiling has been associated with improved long-term outcomes and lower rates of recurrence compared to traditional endovascular coiling alone.[11,12]

However, it is important to highlight that the use of stents in aneurysm treatment is a complex decision that must be made on a case-by-case basis, taking into consideration various factors including aneurysm morphology, patient characteristics, and the expertise of the treating physicians. In addition, further research and clinical studies are necessary to fully understand the long-term outcomes and potential complications associated with stent-induced aneurysm deformation.[13,14]

In conclusion, the concept of stent-induced aneurysm deformation represents a promising approach in the treatment of patients with saccular cerebral aneurysms located in the ICA. By altering the hemodynamics and promoting aneurysm remodeling, this technique offers the potential for enhanced aneurysm stability and reduced risk of rupture. Continued advancements and research in this field have the potential to revolutionize the management of intracranial aneurysms, improving patient outcomes and quality of life.[15–17]

While stent-induced aneurysm deformation has shown promising results in the treatment of cerebral aneurysms, it is important to acknowledge that there are potential complications associated with this approach. During or after stent placement, there is a risk of thrombus formation within the stent or at the site of the aneurysm. This can potentially lead to thromboembolic events, such as stroke, if the blood supply to critical areas of the brain is compromised. Antiplatelet medications are typically prescribed to reduce the risk of thrombus formation. While stent-induced aneurysm deformation aims to promote aneurysm occlusion, there is a possibility of incomplete occlusion. In some cases, the aneurysm may not completely seal off from the circulation, allowing for a residual flow that may increase the risk of future rupture or require additional treatments. Stents may shift or migrate from their intended position after placement. This can affect their ability to induce aneurysm deformation and may require further intervention or repositioning. Stent malpositioning can also lead to inadequate aneurysm occlusion or compromise the parent vessel.[18,19]

Stents themselves can contribute to the development of in-stent stenosis, where the blood vessel narrows within the stent. This can lead to reduced blood flow and potential ischemic events. In rare cases, complete stent occlusion can occur, which may require additional intervention. During stent placement, there is a risk of vessel perforation or dissection, where the arterial wall is damaged or separated. These complications can cause bleeding, compromise blood flow, and necessitate immediate intervention to address the issue. Stents are medical devices, and like any other device, they carry the risk of device-related complications such as allergic reactions, infections, or intolerance to the material used in the stent.[20,21]

It is essential for patients considering stent-assisted aneurysm treatment to have a detailed discussion with their healthcare providers about the potential risks and benefits. The decision to use stent-induced aneurysm deformation should be based on individual patient factors, including the characteristics of the aneurysm, medical history, and the expertise of the treating physicians. Close monitoring and follow-up care are crucial to detect and manage any potential complications that may arise. While stent-induced aneurysm deformation is a relatively newer technique in the treatment of cerebral aneurysms, several studies have investigated its long-term outcomes.[22,23]

One of the primary goals of stent-induced aneurysm deformation is to promote aneurysm occlusion, preventing blood flow into the aneurysm sac. Studies have reported favorable long-term occlusion rates, with many patients achieving complete or near-complete occlusion of the aneurysm over time. This can contribute to a reduced risk of aneurysm rupture and related complications. Stent-induced aneurysm deformation aims to induce aneurysm remodeling and promote the formation of a stable thrombus within the aneurysm sac. Long-term studies have demonstrated that stent-assisted coiling can lead to enhanced aneurysm stability, reducing the risk of future growth or recurrence. This stability is crucial in preventing aneurysm rupture and providing long-term durability of the treatment. While stent-induced aneurysm deformation has shown promising results in reducing aneurysm recurrence rates, it is important to note that the risk of recurrence still exists. Long-term follow-up studies have reported variable rates of aneurysm recurrence, ranging from very low to moderate. The development of recurrence may depend on various factors, including aneurysm characteristics, patient-specific factors, and the type of stent and coiling technique employed. Long-term studies have also evaluated the need for reintervention following stent-induced aneurysm deformation. While the rates of reintervention can vary, several studies have reported relatively low rates of reintervention for aneurysm recurrence or other complications. This suggests that stent-induced aneurysm deformation can provide durable outcomes, reducing the need for additional treatments in many cases.[23,24]

In terms of clinical outcomes, long-term studies have reported favorable results in terms of patient morbidity and mortality. The use of stent-induced aneurysm deformation has been associated with low rates of procedure-related complications, such as stroke or neurologic deficits. Patients generally experience improved clinical outcomes and quality of life following successful treatment of their aneurysms.

It is important to note that the long-term outcomes of stent-induced aneurysm deformation can vary depending on several factors, including patient characteristics, aneurysm morphology, and the specific technique employed. In addition, long-term studies on this specific technique are still relatively limited, and ongoing research and monitoring are necessary to further understand the

durability and potential complications associated with this treatment approach. Individual patient outcomes may also vary, and it is crucial for patients to have thorough discussions with their healthcare providers regarding the expected long-term outcomes, potential risks, and the need for follow-up care.[25]

In this paper, the applied deformation by the stent is investigated and simulated via computational fluid dynamics. The primary outline of this work is rupture risk evaluation on the aneurysm wall via a comparison of the blood characteristics on the sac surface. Three ICA aneurysms are chosen with the same geometrical feature to offer more reliable data. Two stages of aneurysm deformation are produced while it is assumed that the usage of the stent aligned the parent vessel and reduced the blood flow into the aneurysm domain.

II. COMPUTATIONAL MODELING AND GOVERNING EQUATIONS

The simulation of pulsatile blood hemodynamics is done via the computational fluid dynamic method. The interaction of the blood and vessel is modeled via a one-way Fluid–Solid Interaction (FSI) approach that considers force from blood flow on the vessel wall. Navier–Stokes equations are used for the simulation of the blood flow along the parent vessel and aneurysms. The blood flow is assumed non-Newtonian and incompressible, and the viscosity of the blood could be estimated via different formulas. In this work, the Casson model is chosen for the viscosity characteristics of the blood.[24,25] We used a correlation for calculation of the viscosity (Casson model) in relation with Hematocrit value as follows:

$$\mu = 0.1\left(\left[\sqrt{\eta} + \sqrt{\tau_y\left(\frac{1-e^{-m|\dot{\gamma}|}}{|\dot{\gamma}|}\right)}\right]^2\right) \text{ and } \tau_y = (0.625H)^3, \quad (1)$$

where H represents the hematocrit value of the blood.

The selection of the aneurysms is done via a comparison of the available geometries of ICA aneurysms on the Aneurisk webpage.[26] ANSYS-FLUENT is used for hemodynamic modeling.[27] In fact, the three chosen models (Fig. 1) have identical geometrical

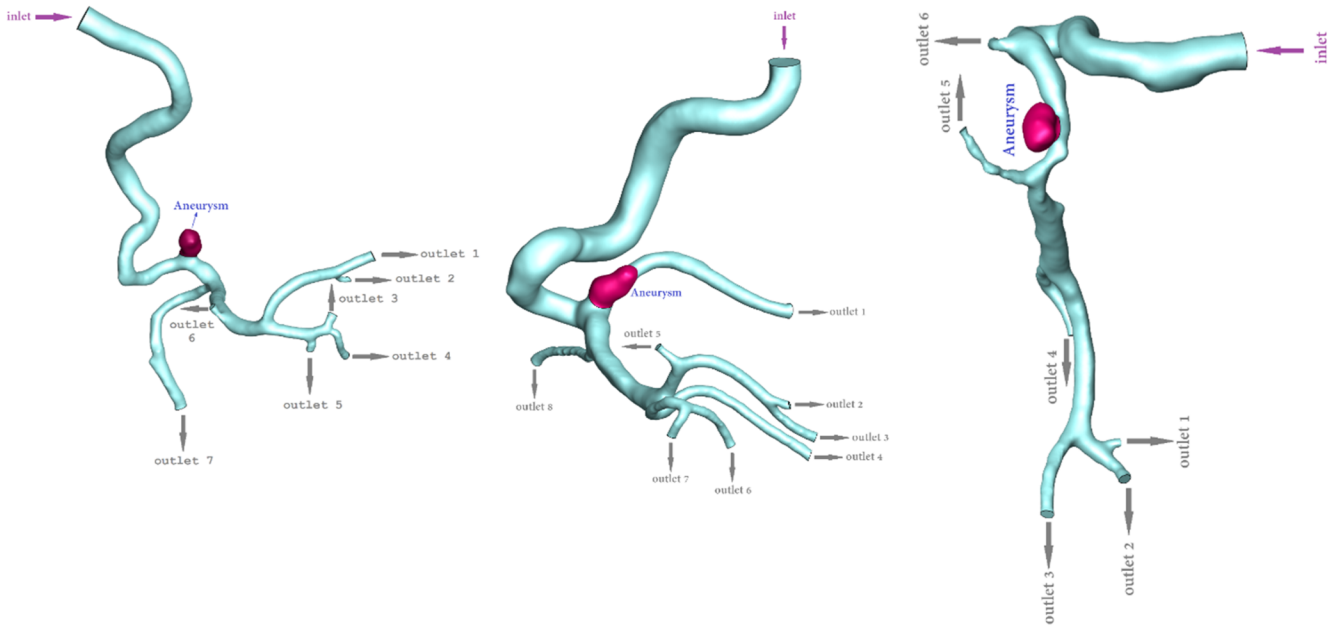

FIG. 1. Geometry of ICA: (a) model A, (b) model B, and (c) model C.

TABLE I. Details of selected ICA patients.

Case ID	Age (year)	Sex	Sac volume (mm^3)	Sac surface area (mm^2)	Sac ellipsoid volume (mm^3)	Sac ellipsoid max semi axis (mm)	Ellipsoid min semi axis (mm)	Sac ostium section perimeter (mm)	Sac ostium shape factor	Sac vessel diameter (mm)
A	26	Female	37.93	54.84	25.17	2.52	1.47	9.52	0.7	2.19
B	53	Male	42.81	61.96	25.67	3.19	1.34	10.84	0.7	2.46
C	47	Male	35.66	51.81	26.74	2.51	1.41	8.15	0.73	1.97

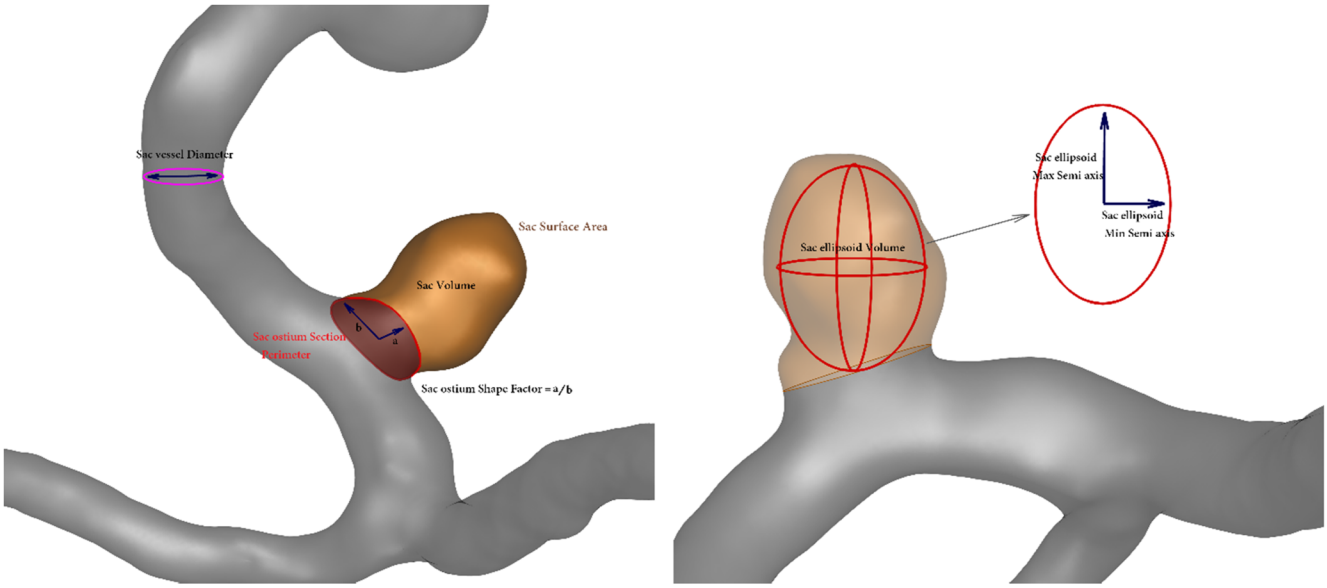

FIG. 2. Geometry of information.

features to authenticate the archived hemodynamic results. Table I presents the details of these chosen ICA aneurysms for this study. The table shows that the change in geometrical features is less than 10% in these cases. The definition of these geometrical characteristics is also displayed in Fig. 2. As mentioned, the main scope is to examine the aneurysm deformation on the hemodynamics. Since the aneurysm deformation is the main outcome of stent usage, two deformed stages have been introduced to capture the trend of hemodynamic change under the impacts of the stent deformation. As shown in Fig. 3, the parent vessel is fully aligned in the second

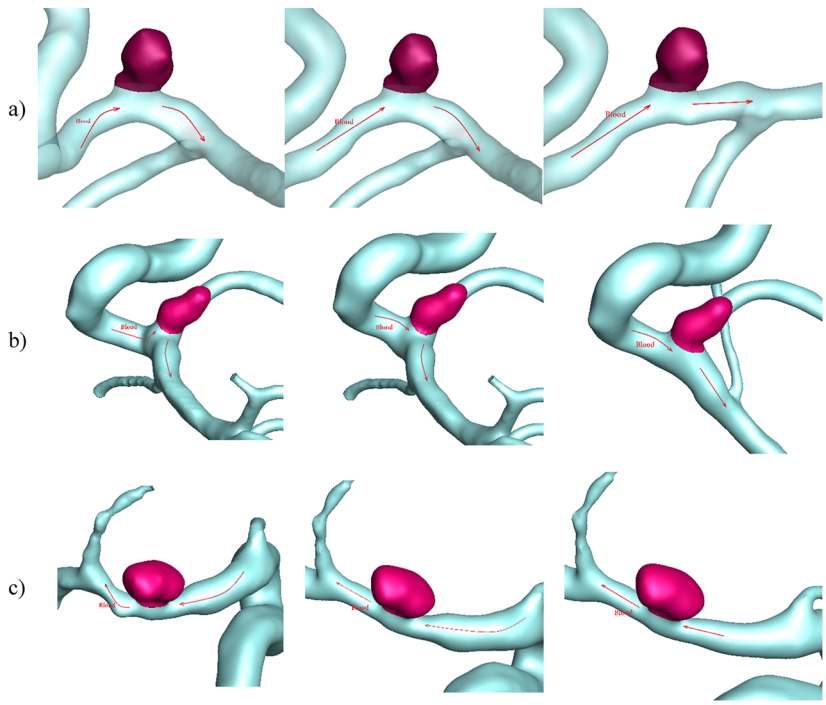

FIG. 3. Geometry of ICA models and their deformations: (a) model A, (b) model B, and (c) model C.

stage of deformation. The size of the aneurysm and the parent vessel remains constant while just the angle is assumed to be changed after deformation.

The pulsatile blood flow is modeled by the applied cardiac cycle at the inlet and outlet as presented in Fig. 4. Figure 4 illustrates the mass flow rate of blood through a specific vessel over the course of a cardiac cycle. The peak mass flow rate corresponds to the systolic phase when the heart pumps blood forcefully, increasing the velocity of blood through the arteries. Conversely, the lower mass flow rate observed during diastole reflects the reduced velocity as the heart relaxes. Given a constant cross-sectional area, these variations in mass flow rate directly reflect changes in blood velocity, which are consistent with physiological expectations. The density of blood, assumed to be 1060 kg/m^3, remains constant, reinforcing the proportional relationship between velocity and mass flow rate. While pressure is applied at the outlet, the mass flow rate is employed at the inlet.[28,29] The selected cycle is related to normal body conditions and

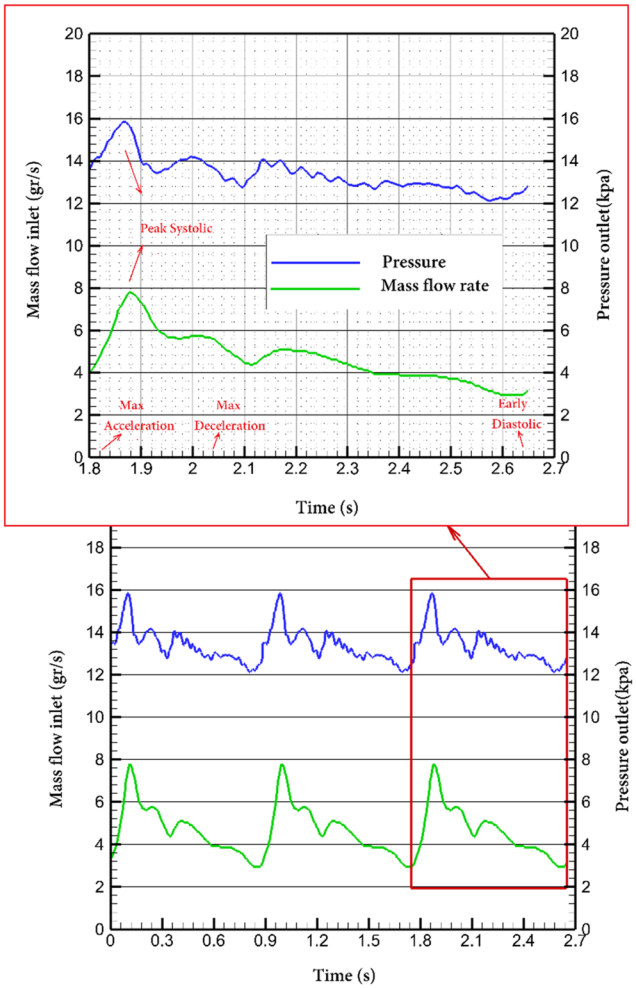

FIG. 4. Applied mass and pressure profile at inlet and outlets.

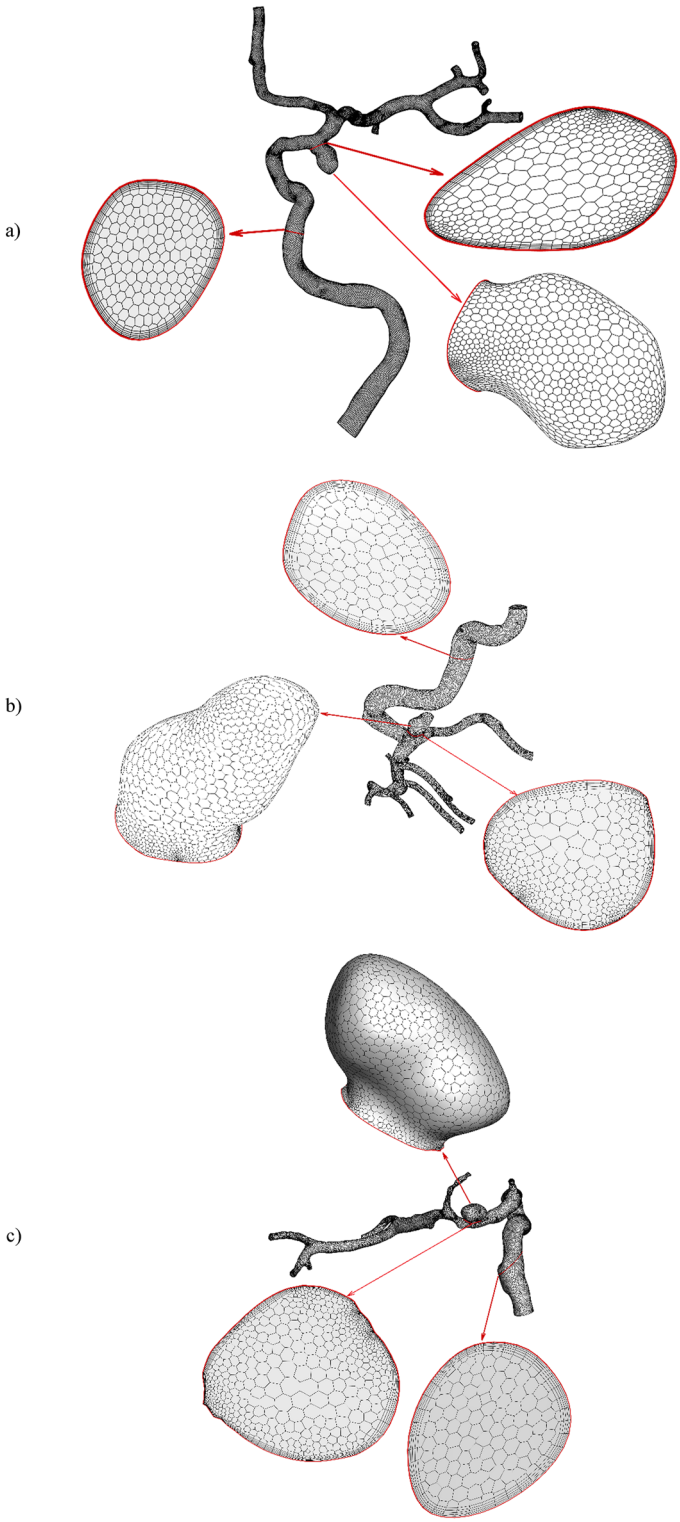

FIG. 5. Grid generation for geometry: (a) model A, (b) model B, and (c) model C.

the main stages of this cycle are also specified in Fig. 4. Three cycles are simulated to ensure the correctness of the obtained data.[30–32] The peak systolic is the stage where the maximum blood flow rate happens, and this critical stage is selected for all hemodynamic factors except Oscillatory Shear Index (OSI) that should calculate at end of the cardiac cycle. The calculation of OSI should be done for the whole cycle of cardiac through the following equation:

$$OSI = \frac{1}{2}\left(1 - \frac{\left|\int_0^T WSS_i dt\right|}{\int_0^T |WSS_i| dt}\right). \quad (2)$$

The produced grids for the selected models after extensive grid study are displayed in Fig. 5. The main difficulty of the grid production for such complex geometry is related to the region close to the main sac region that is the main attention of this work. In addition, the aneurysm deformation requires new grids, and this work tried to offer similar grid size and resolution for the produced domain Ref. 33. A tetrahedral grid is generated for the selected ICA cases, and the resolution of the generated grid near the vessel and aneurysm wall is higher to improve the precision of blood flow feature in this region for the calculation of the hemodynamic factors. Indeed, the boundary late is produced near the wall as depicted in Fig. 5.

III. RESULTS AND DISCUSSION

Figure 6 demonstrates the contour of the wall shear stress on the surface of the aneurysms at peak systolic. The contour of Wall Shear Stress (WSS) shows where the WSS value is critical and rupture risk is possible. In models A and C, the contour of WSS does not show a specific trend after deformations. However, the reduction in the magnitude of the WSS on the sac surface of model B is noticeable. The influence of the deformation on the mean WSS on the sac surface for three selected cases is displayed in Fig. 7. While aneurysm

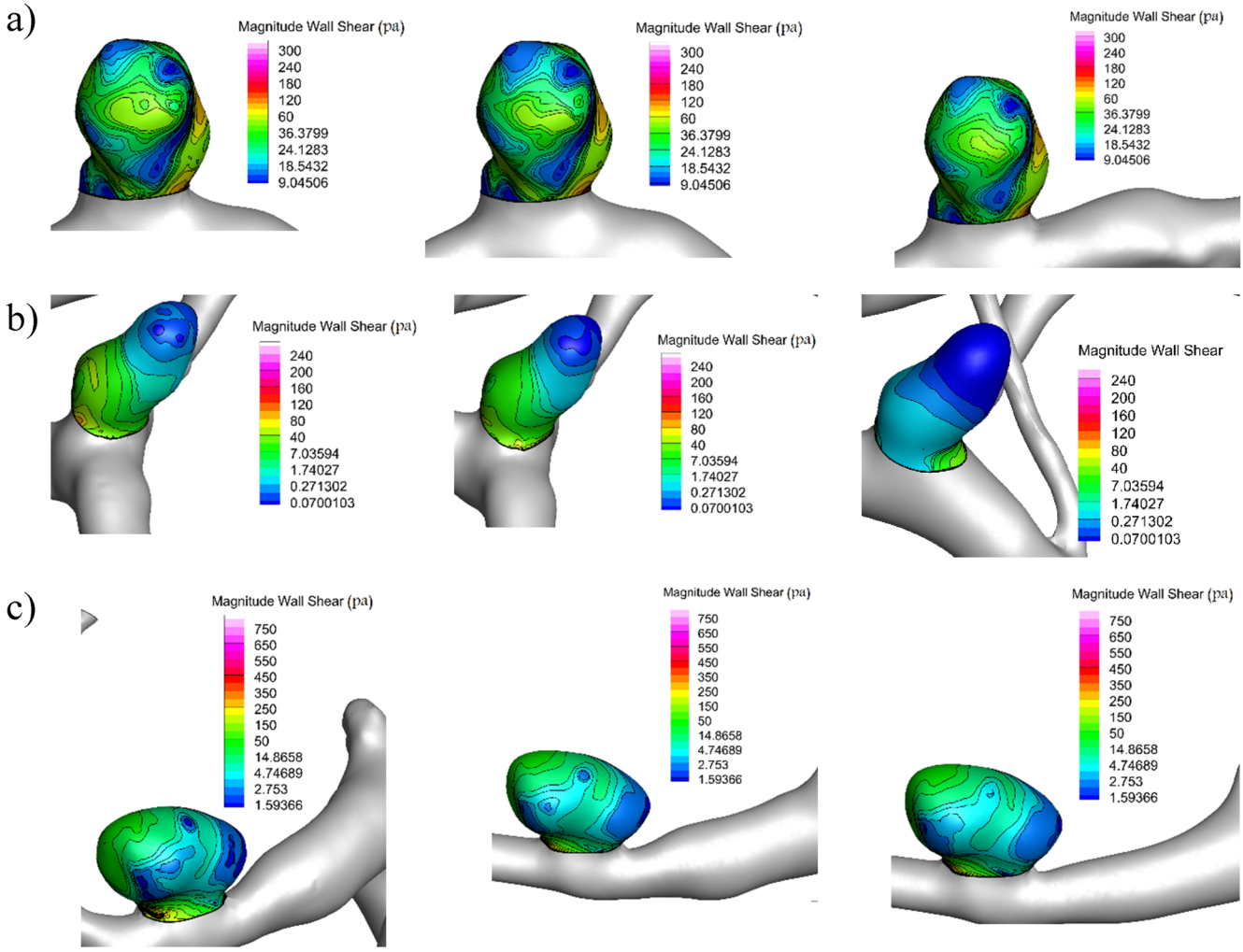

FIG. 6. WSS contours (peak systolic) in the base case, first deformation, and second deformation: (a) model A, (b) model B, and (c) model C.

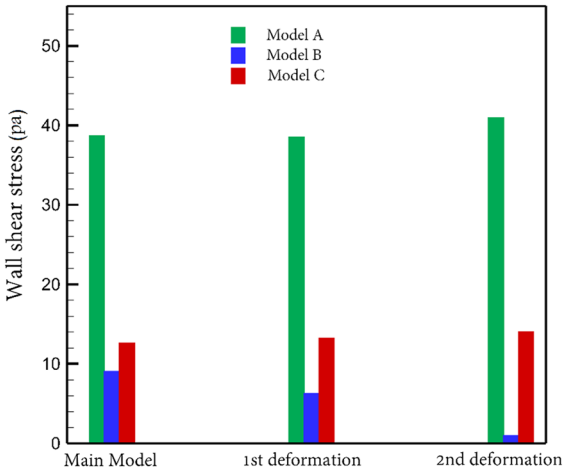

FIG. 7. Deformation effects on mean WSS.

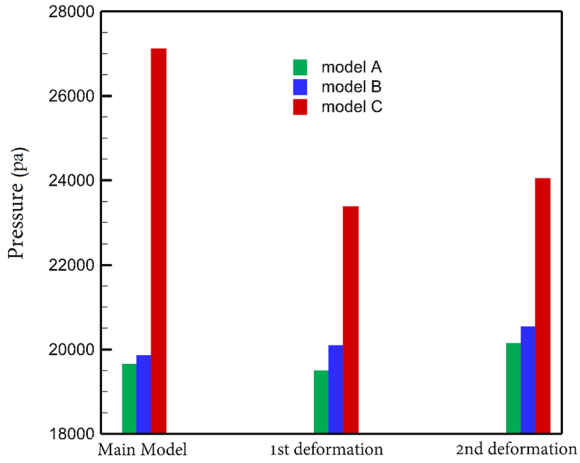

FIG. 9. Deformation effects on mean sac wall's pressure.

deformation does not reduce the mean wall shear stress in models A and C, the meaningful reduction in the mean WSS of model B is noticed. This expressive change may be related to the alignment of the sac's normal plane and parent vessel axis. Thus, deformation of the aneurysms effectively changes the blood flow direction and reduces the risk of rupture in this model.

In Fig. 8, the variations of the pressure on the sac surface under the influence of two deformation stages are displayed. The presented

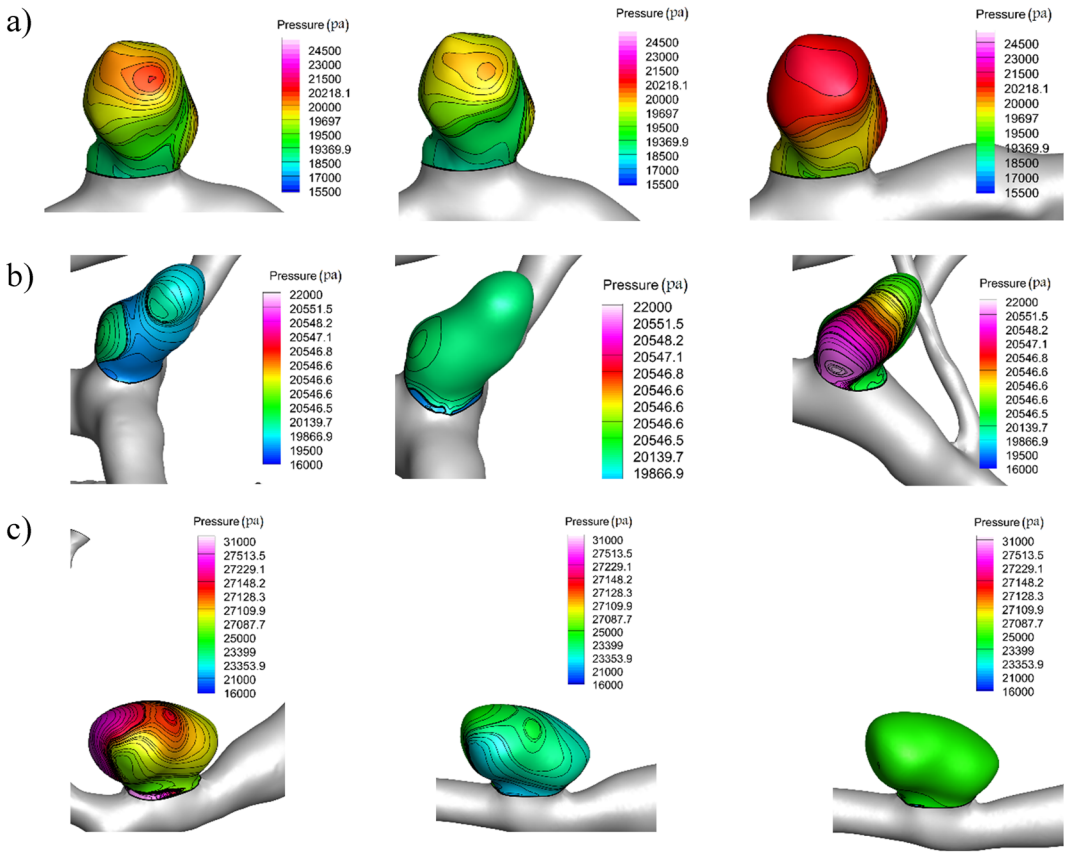

FIG. 8. Pressure contours (peak systolic) in the base case, first deformation, and second deformation: (a) model A, (b) model B, and (c) model C.

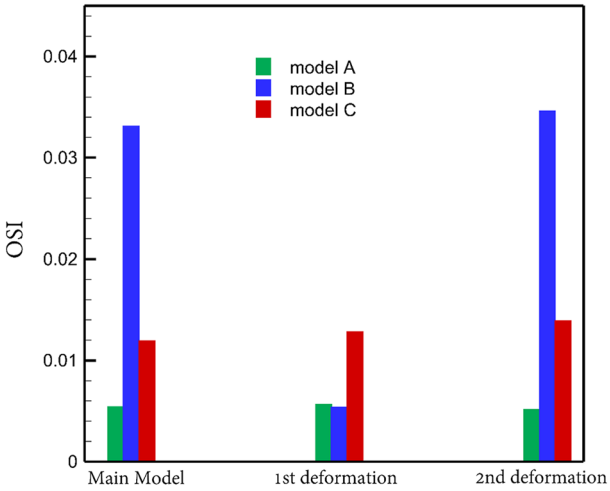

FIG. 11. Deformation effects on mean OSI.

pressure data indicate that the deformation change does not result in a meaningful reduction in the pressure distribution on the wall of the aneurysms. A quantitative comparison of the pressure value on the surface of the aneurysm (Fig. 9) also confirms that the deformation does not change the mean pressure value over the whole sac domain although it may change the pressure locally as noted in Fig. 8. The results indicate that the pressure value of model C is higher than that of other models.

The oscillatory of the blood flow inside the cerebral aneurysm is also important for the evaluation of the aneurysm rupture. This work investigates the value of the OSI for the detection of the potential region for hemorrhage as shown in Fig. 10. As mentioned before, the OSI index is calculated at early diastolic. The change in this important parameter indicates that the most decrease in the OSI index happens in model B. Indeed, the deformation of the aneurysm effectively reduces the OSI by redirection of the blood flow into the main parent vessel. A comparison of OSI on dome and ostium sections also shows that ostium is an important section since the value of OSI is higher in this region. Figure 11 presents the data associated

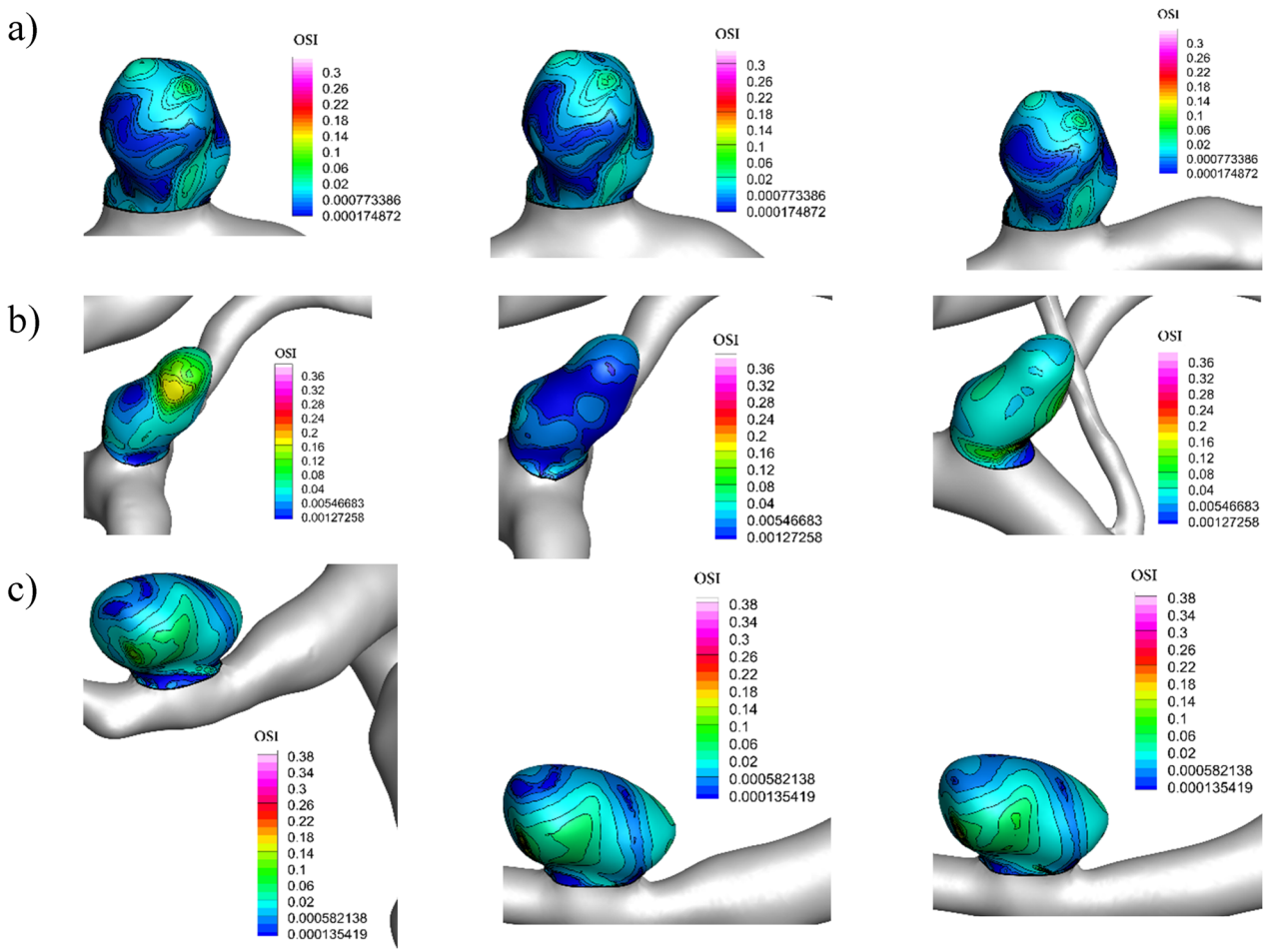

FIG. 10. OSI contours (peak systolic) in the base case, first deformation, and second deformation: (a) model A, (b) model B, and (c) model C.

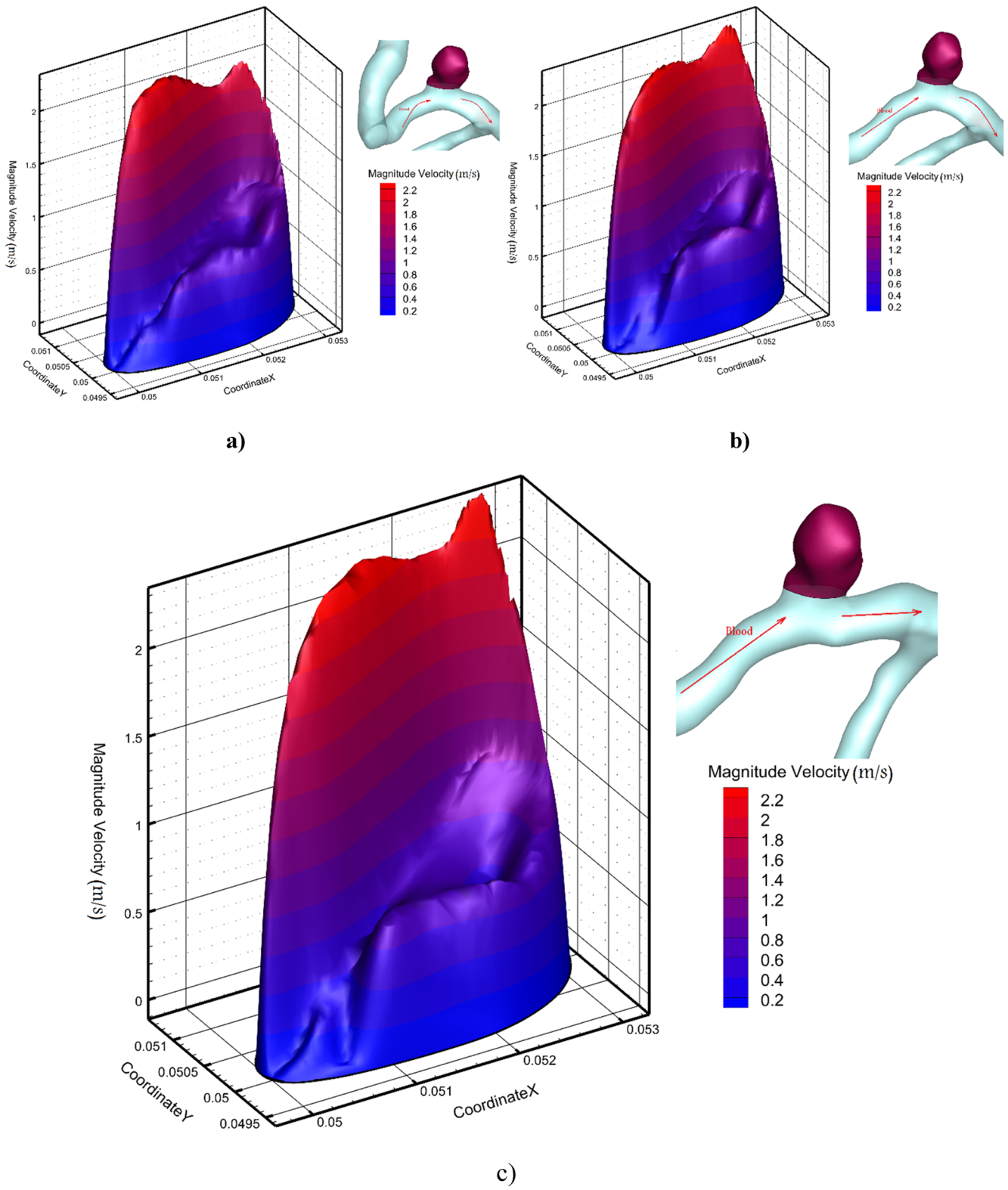

FIG. 12. The effect of deformation on axial velocity distribution for model A: (a) main model, (b) first deformation, and (c) second deformation.

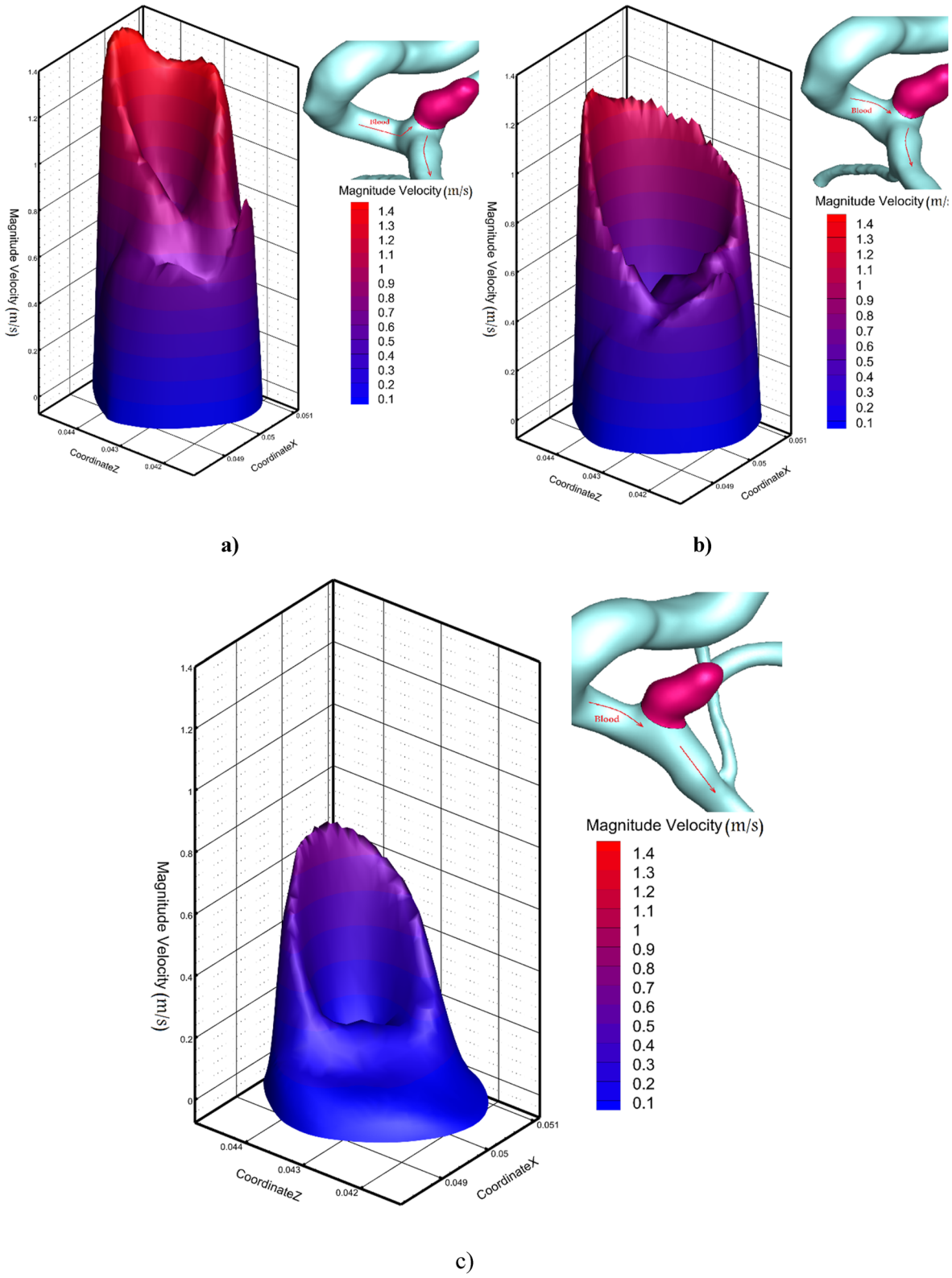

FIG. 13. The effect of deformation on axial velocity distribution for model B: (a) main model, (b) first deformation, and (c) second deformation.

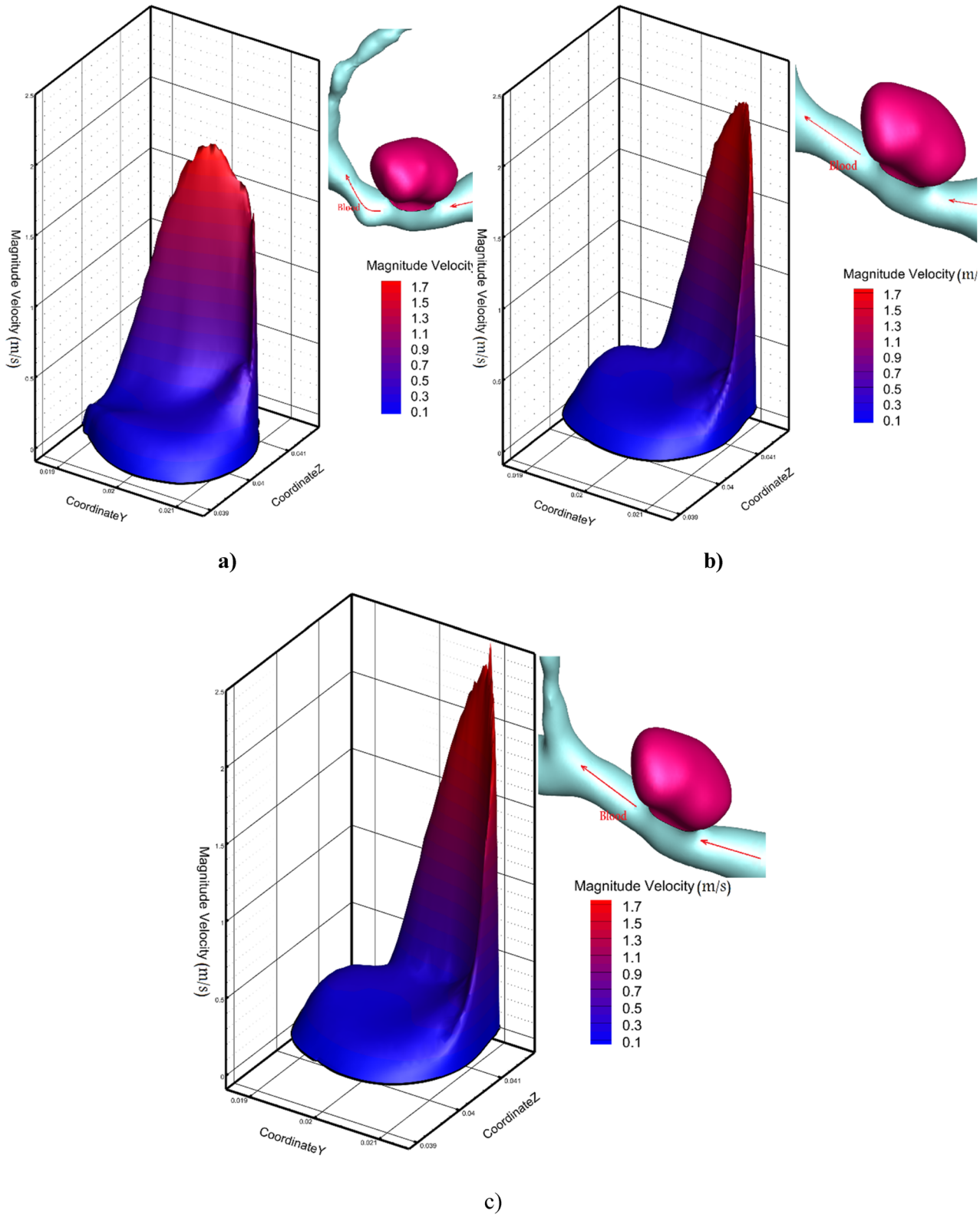

FIG. 14. The effect of deformation on axial velocity distribution for model C: (a) main model, (b) first deformation, and (c) second deformation.

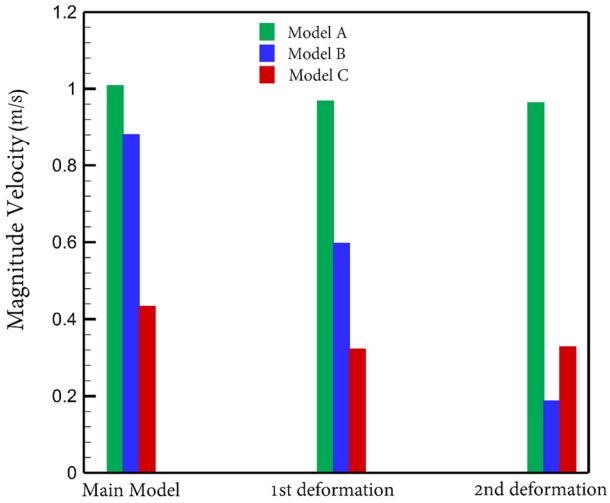

FIG. 15. Deformation effects on mean velocity through ostium neck.

with the mean OSI value for these cases after and before deformations. Based on the value of mean OSI, deformation changes the deformations profoundly.

The main deformation effect could be noticed via a comparison of the velocity profile at the ostium section. The velocity profile of the original cases and deformed aneurysms is demonstrated in Figs. 12–14. In Fig. 12, the change in the velocity profile at the ostium section shows that the deformation has limited effects on the velocity profile. The deformation of the aneurysm in model B decreases the maximum value of the velocity profile, and the blood flow enters into the sac section with a uniform structure (Fig. 13). The distribution of the velocity after the first deformation confirms a substantial reduction in the magnitude of the velocity. The second stage of deformation also reduces the velocity magnitude of the blood flow entering the aneurysm sac region. Unlike cases A and B, the deformation of the aneurysm did not change the maximum value of the velocity in model C. Although the average velocity of the blood entering the sac region decreases, the creeping feature of the blood flow is also augmented in this model after deformation as demonstrated in Fig. 14. The value of the mean blood velocity

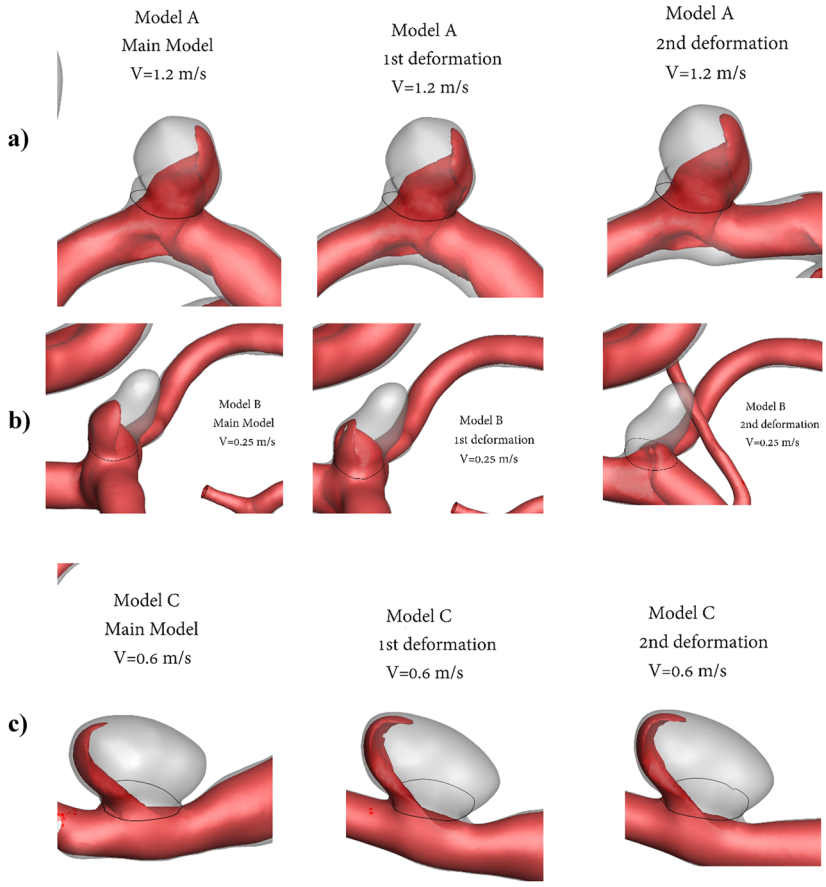

FIG. 16. Iso-surface in the base case, first deformation, and second deformation: (a) model A, (b) model B, and (c) model C.

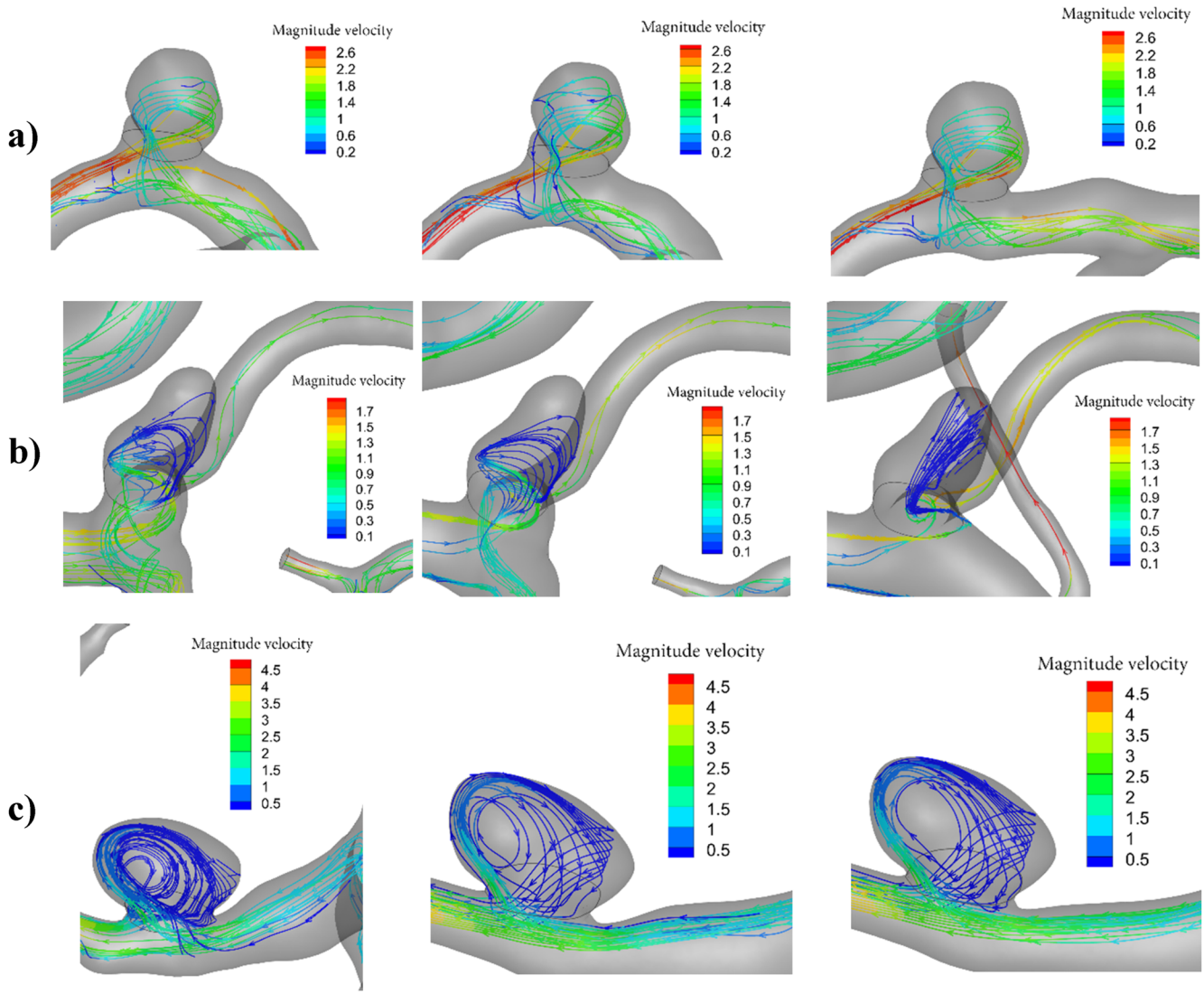

FIG. 17. Streamlines (peak systolic) in the base case, first deformation, and second deformation: (a) model A, (b) model B, and (c) model C.

confirms that the magnitude of the velocity decreases just for model B while mean velocity did not change in other cases (Fig. 15).

The structure of the blood flow inside the presented saccular aneurysms with/without deformations is displayed in Fig. 16. The iso-velocity surface with specific velocity magnitude is displayed to disclose the change induced by deformation inside the cerebrovascular aneurysms. This figure clearly demonstrates how deformation deflects the blood flow into the main parent vessel after deformation, especially in model B. Indeed, the deformation of an aneurysm in this model reduces the velocity and less blood flow enters to saccular region. Figure 17 demonstrates the stream of the blood inside the deformed and original models to compare the stream change induced by the aneurysm deformations. To note the main effects of aneurysm deformation, the streamline of the blood is colored by the velocity magnitude. In the ostium section, the blood flow has a maximum velocity, and a meaningful velocity reduction is observed after the first contact of the blood flow with the aneurysm wall. The circulation of the blood flow almost covers the whole aneurysm section especially for models with semi-circular shapes. In model B, limited blood flow circulated inside the saccular domain, and consequently, the velocity and wall shear stress in this model are lower than those in other cases due to the non-circular shape of this aneurysm.

IV. CONCLUSION

This study has focused on the hemodynamic change induced by the usage of stents inside the three ICA aneurysms. This work presents a comprehensive hemodynamic evaluation of blood flow

within the saccular ICA aneurysms after and before deformation caused by the usage of the stent. Three saccular aneurysms with real specifications are chosen for the evaluation of the hemodynamic factors of WSS, pressure, and OSI. To simulate blood inside these models, the finite volume computational fluid dynamic technique is employed with the Casson model for the calculation of the blood viscosity. The results of the computational investigation disclose that the deformation created by the stent usage decreases the shear stress and OSI in the case when the normal angle of the ostium plane is aligned with the axis of the parent vessel. The comparison of the velocity magnitude of deformed cases with the original also shows how the blood flow is limited by the deformation of the aneurysms. Our study shows that the deformation of the aneurysm is effective, especially when the angle of the sac ostium is high. Meanwhile, deformation induced by the stent reduces the wall shear stress due to the limitation of blood inflow to the sac domain. In addition, the magnitude of the blood velocity was reduced by about 50% by the deformation of the parent vessel.

ACKNOWLEDGMENTS

The authors acknowledged support from Portuguese National Funds by FCT—Foundation for Science and Technology, I.P., within the unit C-MAST - UIDB/00151/2020 (https://doi.org/10.54499/UIDB/00151/2020) and UIDP/00151/2020 (https://doi.org/10.54499/UIDP/00151/2020).

AUTHOR DECLARATIONS

Conflict of Interest

The authors have no conflicts to disclose.

Author Contributions

S Valiallah Mousavi: Conceptualization (equal); Methodology (equal). **M. Barzegar Gerdroodbary**: Methodology (equal); Writing – original draft (equal). **Amir Sabernaeemi**: Software (equal); Validation (equal). **Sajad Salavatidezfouli**: Methodology (equal); Resources (equal); Software (equal). **Peiman Valipour**: Investigation (equal); Methodology (equal); Writing – original draft (equal).

DATA AVAILABILITY

All data generated or analyzed during this study are included in this published article.

REFERENCES

[1] A. Rostamian, K. Fallah, and Y. Rostamiyan, "Reduction of rupture risk in ICA aneurysms by endovascular techniques of coiling and stent: Numerical study," Sci. Rep. **13**, 7216 (2023).
[2] P. Valipour, "Effects of coiling embolism on blood hemodynamic of the MCA aneurysm: A numerical study," Sci. Rep. **12**(1), 22029 (2022).
[3] A. Rostamian, K. Fallah, Y. Rostamiyan, and J. Alinejad, "Computational study of the blood hemodynamic inside the cerebral double dome aneurysm filling with endovascular coiling," Sci. Rep. **13**(1), 2909 (2023).
[4] A. Rostamian, K. Fallah, Y. Rostamiyan, and J. Alinejad, "Application of computational fluid dynamics for detection of high risk region in middle cerebral artery (MCA) aneurysm," Int. J. Mod. Phys. C **34**, 2350019 (2022).
[5] K. Valen-Sendstad, A. W. Bergersen, Y. Shimogonya, L. Goubergrits, J. Bruening, J. Pallares, S. Cito *et al.*, "Real-world variability in the prediction of intracranial aneurysm wall shear stress: The 2015 international aneurysm CFD challenge," Cardiovasc. Eng. Technol. **9**, 544–564 (2018).
[6] H. Jiang, Z. Lu, M. B. Gerdroodbary, A. Sabernaeemi, and S. Salavatidezfouli, "The influence of sac centreline on saccular aneurysm rupture: Computational study," Sci. Rep. **13**(1), 11288 (2023).
[7] G. D. Maher, C. M. Fleeter, D. E. Schiavazzi, and A. L. Marsden, "Geometric uncertainty in patient-specific cardiovascular modeling with convolutional dropout networks," Comput. Methods Appl. Mech. Eng. **386**, 114038 (2021).
[8] Y. Hoi, H. Meng, S. H. Woodward, B. R. Bendok, R. A. Hanel, L. R. Guterman, and L. N. Hopkins, "Effects of arterial geometry on aneurysm growth: Three-dimensional computational fluid dynamics study," J. Neurosurg. **101**, 676–681 (2004).
[9] S. Sankaran, L. Grady, and C. A. Taylor, "Impact of geometric uncertainty on hemodynamic simulations using machine learning," Comput. Methods Appl. Mech. Eng. **297**, 167–190 (2015).
[10] C. Zhang, H. Ge, S. Zhang, D. Liu, Z. Jiang, C. Lan, L. Li, H. Feng, and R. Hu, "Hematoma evacuation via image-guided para-corticospinal tract approach in patients with spontaneous intracerebral hemorrhage," Neurol. Ther. **10**(2), 1001–1013 (2021).
[11] P. C. Fu, J. Y. Wang, Y. Su, Y. Q. Liao, S. L. Li, G. L. Xu, Y. J. Huang, M. H. Hu, and L. M. Cao, "Intravascular ultrasonography assisted carotid artery stenting for treatment of carotid stenosis: Two case reports," World J. Clin. Cases **11**(29), 7127–7135 (2023).
[12] R. Huo, Y. Liu, H. Xu, J. Li, R. Xin, Z. Xing, S. Deng, T. Wang, H. Yuan, and X. Zhao, "Associations between carotid atherosclerotic plaque characteristics determined by magnetic resonance imaging and improvement of cognition in patients undergoing carotid endarterectomy," Quant. Imaging Med. Surg. **12**(5), 2891–2903 (2022).
[13] B. Shen, S. Xiao, C. Yu, C. Zhang, J. Zhan, Y. Liu, and W. Fu, "Cerebral hemodynamics underlying ankle force sense modulated by high-definition transcranial direct current stimulation," Cereb. Cortex **34**(6), bhae226 (2024).
[14] I. Chatziprodromou, V. Butty, V. B. Makhijani, D. Poulikakos, and Y. Ventikos, "Pulsatile blood flow in anatomically accurate vessels with multiple aneurysms: A medical intervention planning application of computational haemodynamics," Flow, Turbul. Combust. **71**, 333–346 (2003).
[15] X. Y. Shen, M. Barzegar Gerdroodbary, A. M. Abazari, and R. Moradi, "Computational study of blood flow characteristics on formation of the aneurysm in internal carotid artery," Eur. Phys. J. Plus **136**(5), 541 (2021).
[16] I. Shiryanpoor, P. Valipour, M. Barzegar Gerdroodbary, A. M. Abazari, and R. Moradi, "Using computational fluid dynamic for evaluation of rupture risk of micro cerebral aneurysms in the growth process: Hemodynamic analysis," Int. J. Mod. Phys. C (published online, 2024).
[17] Y. C. Fung, *Biomechanics: Mechanical Properties of Living Tissues*, 2nd ed. (Springer, Boston, 1993).
[18] A. Razavi, E. Shirani, and M. Sadeghi, "Numerical simulation of blood pulsatile flow in a stenosed carotid artery using different rheological models," J. Biomech. **44**, 2021–2030 (2011).
[19] S. Salavatidezfouli, A. Alizadeh, M. Barzegar Gerdroodbary, A. Sabernaeemi, A. M. Abazari, and A. Sheidani, "Investigation of the stent induced deformation on hemodynamic of internal carotid aneurysms by computational fluid dynamics," Sci. Rep. **13**(1), 7155 (2023).
[20] A. Sadeh, A. Kazemi, M. Bahramkhoo, and M. Barzegar Gerdroodbary, "Computational study of blood flow inside MCA aneurysm with/without endovascular coiling," Sci. Rep. **13**, 4560 (2023).
[21] M. Mirzaei Poueinak, S. A. Abdollahi, A. Alizadeh, M. A. Youshanlui, H. Zekri, and M. B. Gerdroodbary, "Computational study of blood hemodynamic in ICA aneurysm with coiling embolism," Int. J. Mod. Phys. C **34**(10), 2350138 (2023).
[22] A. Sabernaeemi, M. Barzegar Gerdroodbary, S. Salavatidezfouli, and P. Valipour, "Influence of stent-induced vessel deformation on hemodynamic feature of bloodstream inside ICA aneurysms," Biomech. Model. Mechanobiol. **22**, 1193 (2023).

[23]S. Hariri, M. Mirzaei Poueinak, A. Hassanvand, M. Barzegar Gerdroodbary, and M. Faraji, "Effects of blood hematocrit on performance of endovascular coiling for treatment of middle cerebral artery (MCA) aneurysms: Computational study," Interdiscip. Neurosurg. **32**, 101729 (2023).
[24]Z.-H. Jin, M. Barzegar Gerdroodbary, P. Valipour, M. Faraji, and N. H. Abu-Hamdeh, "CFD investigations of the blood hemodynamic inside internal cerebral aneurysm (ICA) in the existence of coiling embolism," Alexandria Eng. J. **66**, 797 (2023).
[25]A. Sheidani, M. Barzegar Gerdroodbary, A. Poozesh, A. Sabernaeemi, S. Salavatidezfouli, and A. Hajisharifi, "Influence of the coiling porosity on the risk reduction of the cerebral aneurysm rupture: Computational study," Sci. Rep. **12**, 19082 (2022).
[26]AneuriskWeb project website, http://ecm2.mathcs.emory.edu/aneuriskweb, Emory University, Department of Math&CS, 2012.
[27]Ansys, Inc., ANSYS® Fluent User's Guide, Release 2020 R2, ANSYS, Canonsburg, 2020.
[28]S. Voß, O. Beuing, G. Janiga, and P. Berg, "Stent-induced vessel deformation after intracranial aneurysm treatment—A hemodynamic pilot study," Comput. Biol. Med. **111**, 103338 (2019).
[29]S. Qin, B. Wu, J. Liu, W.-S. Shiu, Z. Yan, R. Chen, and X.-C. Cai, "Efficient parallel simulation of hemodynamics in patient-specific abdominal aorta with aneurysm," Comput. Biol. Med. **136**, 104652 (2021).
[30]L. Xu, F. Liang, B. Zhao, J. Wan, and H. Liu, "Influence of aging-induced flow waveform variation on hemodynamics in aneurysms present at the internal carotid artery: A computational model-based study," Comput. Biol. Med. **101**, 51–60 (2018).
[31]A. Boccadifuoco, A. Mariotti, S. Celi, N. Martini, and M. V. Salvetti, "Impact of uncertainties in outflow boundary conditions on the predictions of hemodynamic simulations of ascending thoracic aortic aneurysms," Comput. Fluids **165**, 96–115 (2018).
[32]A. P. Mitsos, N. M. P. Kakalis, Y. P. Ventikos, and J. V. Byrne, "Haemodynamic simulation of aneurysm coiling in an anatomically accurate computational fluid dynamics model: Technical note," Neuroradiology **50**(4), 341–347 (2008).
[33]M. Malvè, S. Chandra, A. García, A. Mena, M. A. Martínez, E. A. Finol, and M. Doblaré, "Impedance-based outflow boundary conditions for human carotid haemodynamics," Comput. Methods Biomech. Biomed. Eng. **17**(11), 1248–1260 (2014).